Applied Surface Science 258 (2012) 6266–6271

Contents lists available at SciVerse ScienceDirect

Applied Surface Science

journal homepage: www.elsevier.com/locate/apsusc

Analysis of plasma-mediated ablation in aqueous tissue

Jian Jiao, Zhixiong Guo*

Department of Mechanical and Aerospace Engineering, Rutgers, The State University of New Jersey, Piscataway, NJ 08854, USA

ARTICLE INFO

Article history:
Received 23 September 2011
Received in revised form 25 January 2012
Accepted 4 March 2012
Available online 21 March 2012

Keywords:
Ablation
Ultrafast laser
Biological tissue

ABSTRACT

Plasma-mediated ablation using ultrafast lasers in transparent media such as aqueous tissues is studied. It is postulated that a critical seed free electron density exists due to the multiphoton ionization in order to trigger the avalanche ionization which causes ablation and during the avalanche ionization process the contribution of laser-induced photon ionization is negligible. Based on this assumption, the ablation process can be treated as two separate processes – the multiphoton and avalanche ionizations – at different time stages; so that an analytical solution to the evolution of plasma formation is obtained for the first time. The analysis is applied to plasma-mediated ablation in corneal epithelium and validated via comparison with experimental data available in the literature. The critical seed free-electron density and the time to initiate the avalanche ionization for sub-picosecond laser pulses are analyzed. It is found that the critical seed free-electron density decreases as the pulse width increases, obeying a $t_p^{-5.65}$ rule. This model is further extended to the estimation of crater size in the ablation of tissue-mimic polydimethylsiloxane (PDMS). The results match well with the available experimental measurements.

1. Introduction

Ultrashort-pulsed (USP) lasers with femtoseconds or picoseconds pulse duration have nowadays emerged as a promising tool for micro/nano-processing of various materials [1–9]. For pulses with duration width $t_p > 1$ ns, the generally accepted picture of material damage involves the heating of conduction band electrons by the incident radiation and transfer of this energy to the lattice. Damage occurs via such conventional heat deposition resulting in melting, boiling and thermal-induced fracture of materials. Because the controlling rate is that of thermal conduction through the lattice, such a heat model predicts a $t_p^{0.5}$ dependence of the threshold fluence upon pulse width t_p, in a reasonably good agreement with experiments in a variety of dielectric materials for short pulses from 100 ps to 10 ns [10]. Du et al. [11] reported that for ultrafast lasers with $t_p < 10$ ps, the damage threshold fluence is greater than the prediction from the $t_p^{0.5}$ scaling rule. Many late experimental measurements [12–14] with such ultrashort pulses confirmed the departure from the $t_p^{0.5}$ scaling rule, leading to the discovery of a new ablation category – the so-called plasma-mediated ablation [15–17].

USP laser induced plasma-mediated ablation has been described as: the interaction of a strong electromagnetic field with electrons in a condensed medium can lead to the generation of free electrons in the conduction band through multiphoton or tunnel ionization [15]. These free charges can subsequently gain sufficient kinetic energy from the electric field by inverse Bremsstrahlung (IBA) absorption to produce a large amount of free electrons – the so-called avalanche ionization [16]. The rapid ionization of the medium leads to plasma formation and a drastic increase of the local absorption coefficient which in turn gives rise to a rapid energy transfer from the radiation field to the material and results in material ablation.

It is commonly recognized that there exists a threshold for plasma-mediated ablation. An ionization rate equation [15] predicts the temporal evolution of free electrons. The threshold is determined as the free-electron density reaches to a critical value [16] – the so-called critical free-electron density. Some initial work to illustrate the underlying mechanisms of the plasma-induced ablation was conducted in pure water. It was concluded that the multiphoton ionization was most likely the pathway for generating at least one seed free electron to initiate the avalanche ionization which is predominant in the ablation process in water [15].

Extensive studies on the determination of plasma-mediated ablation thresholds in other transparent dielectrics have also been conducted [11–13] in the past two decades. To theoretically explain the discrepancy in the ultrashort pulse region, Stuart et al. [12] derived a rate equation based on production via multiphoton ionization, Joule heating, and avalanche ionization. Their model yielded a quantitative agreement with experimental measurements of the damage thresholds for fused silica at 526 and 1053 nm for pulses in a wide range from 140 fs to 1 ns. Later Tien et al. [13] developed another rate equation consisting of

* Corresponding author. Tel.: +1 732 4452024.
E-mail address: guo@jove.rutgers.edu (Z. Guo).

0169-4332/$ – see front matter © 2012 Elsevier B.V. All rights reserved.
doi:10.1016/j.apsusc.2012.03.019

Thornber's expression for avalanche ionization and Keldysh's photoionization theory to model single-shot laser ablation, in which the discrepancy from the $t_p^{0.5}$ scaling rule was found in their damage-threshold measurements in the ablation experiments of fused silica at 800 nm in a wide pulse duration range from 10 ns down to 20 fs.

Such discrepancy has also been confirmed by Giguere et al. [18] who conducted experiments on measuring the ablation thresholds on two corneal layers – the epithelium and the stroma – with laser pulse duration from 5 ps down to 100 fs. It was found that the ablation threshold decreased rapidly with pulse durations when pulse width was greater than 1 ps. However, when the pulse width decreased to a value smaller than 1 ps, the ablation threshold did not decrease with the further decease of pulse width. Instead, a roughly constant ablation threshold was observed for pulses with duration width between 100 fs and 1 ps.

By adopting the rate equation, some authors used only one seed free electron produced via multiphoton ionization in the focal volume to initiate avalanche ionization in their calculations [15–17]. As we know, it is very easy to generate a free electron at the focus of a highly intensified laser beam when the photon energy is close to the medium band gap. However, plasma-mediated ablation occurs only when the laser irradiance is over a large threshold value. In other words, we believe that the seed free-electron density must be over a value (critical seed free-electron density) to trigger the avalanche ionization; otherwise, avalanche ionization would occur whenever a pulse irradiation is applied to a medium. Hence, one free electron is not sufficient to trigger the avalanche ionization. To answer the questions that how many seed free electrons are required to trigger avalanche ionization and when avalanche ionization occurs, we focus on establishing a theoretical model which yields an analytical solution for the required seed electron density as a function of pulse width in the present study. Consequently, the triggering time can be obtained once such a critical seed electron density is determined.

In this treatise, plasma-mediated ablation is postulated as two separate processes – the multiphoton and avalanche ionizations – during different time stages; and the rate equation accompanying each process is analytically solved. The critical seed electron density and the time when avalanche ionization occurs to induce ablation in corneal epithelium are analyzed, based on the comparison with the available experimental measurements. This analytical model in combination with the numerical modeling is employed to predict the crater size formed during the USP laser ablation of tissue-mimic polydimethylsiloxane (PDMS) for further validation of our postulation.

2. Model description

A generic rate equation consisting of multiphoton and avalanche ionizations, and diffusion and recombination losses is commonly used to predict the temporal evolution of free electrons (plasmas) in water and aqueous tissues as follows [15–17]:

$$\frac{d\rho}{dt} = \eta_{\mathrm{mp}} + \eta_{\mathrm{ava}}\rho - \eta_{\mathrm{diff}}\rho - \eta_{\mathrm{rec}}\rho^2 \tag{1}$$

where ρ is the plasma density. The first two terms on the right-hand side in the equation represent the production of free electrons through multiphoton and avalanche ionizations, respectively. The last two terms are the electron losses through diffusion and recombination, respectively.

An approximate expression for multiphoton ionization rate η_{mp} in condensed media was derived by Keldysh [19]. For the limiting condition that the optical frequency is much greater than the tunneling frequency, it follows that:

$$\eta_{\mathrm{mp}} \approx \frac{2\omega}{9\pi}\left(\frac{m\omega}{2\hbar}\right)^{3/2}\left[\frac{e^2 I(t)}{8m\Delta E\omega^2 c_0\varepsilon_0 n}\right]^k e^{2k}\Phi\left(\sqrt{2k-\frac{2\Delta E}{\hbar\omega}}\right), \tag{2}$$

in which, $\hbar$ is Dirac constant; ε_0 is the vacuum permittivity; n is the refractive index of the medium; m is the mass of electron; e (=1.6022 × 10^{-19} C) is an electron charge; Φ is the Dawson function; k is the number of photons required to ionize an atom or molecule $k = \langle \Delta E/(\hbar\omega) + 1 \rangle$, and ΔE is the band gap for ionization. The laser circular frequency is $\omega = 2\pi c_0/\lambda$, where c_0 is the speed of light in vacuum.

The avalanche ionization rate coefficient η_{ava} derived by Kennedy for ocular and aqueous media [20] is given as:

$$\eta_{\mathrm{ava}} = \frac{1}{\omega^2\tau^2+1}\left[\frac{e^2\tau}{c_0\varepsilon_0 nm\Delta E}I(t) - \frac{m\omega^2\tau}{M_m}\right] \tag{3}$$

in which, τ (≈1.7 fs [21]) is the time of collision between an electron and a heavy particle, and M_m is the mass of molecule.

The laser irradiance is assumed with a Gaussian profile in both spatial and temporal domains, expressed as:

$$I(t) = (1-R)I_0 \exp\left\{-4\ln 2[(t-t_m)/t_p]^2\right\}\exp\left(\frac{-2r^2}{w_0^2}\right), \tag{4}$$

where I_0 is the peak radiation intensity; t_p is the pulse width at half-maximum; and t_m is the time when the irradiance is in peak. The whole pulse duration is then considered as $t_d = 2t_m$. The beam radius is defined as w_0. It is noticed from the literature that the threshold for plasma-mediated ablation is defined in terms of either peak heat flux or pulse-averaged fluence. To equate these two values, it requires that:

$$\int_0^{t_d} \exp\left[\frac{-4\ \ln 2(t-t_m)^2}{t_p^2}\right] dt = t_p \tag{5}$$

The above equality gives $t_m = 0.79695t_p$. The reflectivity R is calculated by Fresnel equation at the air/material interface.

The decrease of the electron density in the focal volume by diffusion is estimated by approximating the focal volume as a cylinder with beam radius w_0 and Rayleigh length z_R, $z_R = n\pi w_0^2/\lambda$. The diffusion rate per electron is expressed as [15]:

$$\eta_{\mathrm{diff}} = \frac{\tau\Delta E}{3m}\left[\left(\frac{2.4}{w_0}\right)^2 + \left(\frac{1}{z_R}\right)^2\right]. \tag{6}$$

As for the recombination rate in the present study, it is assumed to be $\eta_{\mathrm{rec}} = 2\times10^{-9}$ cm^3/s, an empirical value obtained by Docchio [22] through measurements of the decay of plasma luminescence.

Some previous studies reported that the diffusion and recombination losses could be neglected when the pulse widths were smaller than 10 ps [13]. Therefore, the diffusion and recombination losses are assumed to be negligible in order to obtain an analytical solution of the rate equation. However, these two losses are still incorporated in the numerical modeling in this study to examine our proposed analytical model and solution.

Now based on our postulate that a critical seed free electron density must be achieved through multiphoton ionization only in order to trigger avalanche ionization and during the avalanche ionization process the contribution of multiphoton ionization is negligible, the plasma-mediated ablation process is then split into two separate ionization processes.

First, multiphoton ionization is the only mechanism to generate seed free electrons, i.e.

$$\frac{d\rho}{dt} = \eta_{\mathrm{mp}}, \qquad \text{for} \quad 0 \le t \le t_0. \tag{7}$$

Initially the density is zero. t_0 is the time to trigger avalanche ionization, when the condition holds, i.e. $\rho(t_0)=\rho_0$. Here ρ_0 is introduced for the first time and postulated as the critical seed free-electron density. When the free-electron density is not accumulated to this critical value, no avalanche ionization occurs, i.e., $\eta_{ava}=0$ for $\rho<\rho_0$. Now the seed free electron density $\rho(t)$ at the focus center due to multiphoton ionization is obtained via analytically solving Eq. (7), i.e.,

$$\rho(t) = 0.0133\frac{\omega^{5/2}t_p}{\sqrt{k}}\left(\frac{m}{\hbar}\right)^{3/2}\left(\frac{(1-R)I_0e^2}{8m\Delta E\omega^2c_0\varepsilon_0 n}\right)^k \times \exp(2k)\Phi\left(\sqrt{2k-\frac{2\Delta E}{\hbar\omega}}\right) \times\left\{\mathrm{erf}(1.332\sqrt{k})+\mathrm{erf}\left[\sqrt{k}\left(\frac{1.665t}{t_p}-1.332\right)\right]\right\} \quad (8)$$

Second, once the free electrons are accumulated sufficiently to initialize avalanche ionization, the avalanche ionization is assumed to be dominant thereafter and the contribution due to continuous multiphoton ionization is then negligible. The rate equation in this process is simplified as:

$$\frac{d\rho}{dt}=\eta_{ava}\rho, \qquad \text{for} \quad t_0\le t\le t_d \quad (9)$$

For Eq. (9), the initial condition is $\rho(t_0)=\rho_0$ and the condition of occurrence of ablation is $\rho(t_d)\ge\rho_{cr}$. The critical electron density for optical breakdown (i.e., plasma-mediated ablation) is theoretically defined as [16]:

$$\rho_{cr}=\frac{\omega^2m\varepsilon_0}{e^2} \quad (10)$$

through which we can obtain $\rho_{cr}=1.74\times10^{21}\,\mathrm{cm}^{-3}$ at $\lambda=800$ nm and $\rho_{cr}=4.63\times10^{20}\,\mathrm{cm}^{-3}$ at $\lambda=1552$ nm, respectively.

During the avalanche ionization process, the solution for the time-dependent free electron density $\rho(t)$ at the focus center is:

$$\frac{\rho(t)}{\rho_0}=\exp\left\{A\left[\mathrm{erf}\left(1.665\frac{t}{t_p}-1.332\right)-\mathrm{erf}\left(1.665\frac{t_0}{t_p}-1.332\right)\right]-\frac{m\omega^2\tau}{M_m}\frac{t-t_0}{\omega^2\tau^2+1}\right\} \quad (11a)$$

with

$$A=0.532\frac{(1-R)I_0t_p}{\omega^2\tau^2+1}\frac{e^2\tau}{c_0\varepsilon_0nm\Delta E} \quad (11b)$$

When ablation occurs exactly at the threshold value, there should exist no excessive energy for heat deposition and the whole irradiation should generate a critical free electron density at the end of the pulse, i.e., $\rho(t_d)=\rho_{cr}$. This condition is utilized to determine ρ_0 as well as t_0 from the combined solutions of Eqs. (8), (11a) and (11b). The laser intensity I_0 at ablation threshold is the experimentally measured threshold value.

In the present study, we consider the USP laser plasma-mediated ablation in a corneal epithelium tissue at wavelength 800 nm and in a PDMS sample at wavelength 1552 nm, respectively. For the corneal epithelium, ΔE is taken as 9.0 eV and M_m is assumed as the molecular mass of water 2.99×10^{-26} kg [17]. For the PDMS, ΔE is assumed to be 5.5 eV [23] and $M_m\approx1.99\times10^{-24}$ kg. For the corneal epithelium, $n=1.54$ at wavelength $\lambda=800$ nm; and for the PDMS, $n=1.45$ at wavelength $\lambda=1552$ nm.

3. Results and discussion

We first calculated the ablation threshold induced by laser pulses from 100 fs to 5 ps by using the complete rate equation that consists of multiphoton and avalanche ionizations, and diffusion and recombination simultaneously. In this numerical calculation,

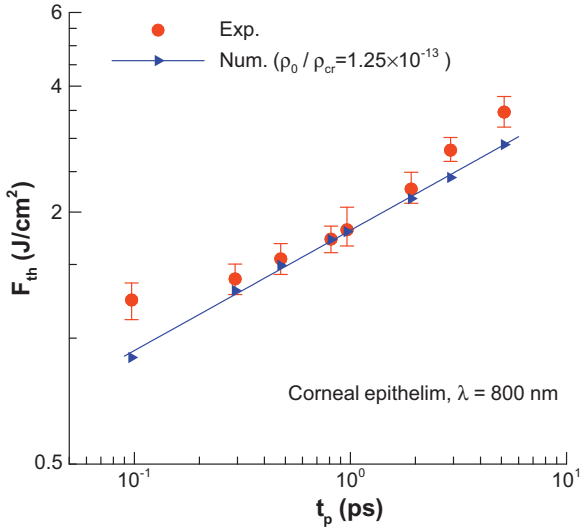

Fig. 1. Fluence thresholds predicted by the numerical model with a single free electron for triggering avalanche ionization (i.e., $\rho_0/\rho_{cr}=1.25\times10^{-13}$) and comparison with experimental data [18] in the literature.

the avalanche ionization is assumed to be initiated when one free electron appears in the focal volume. Both the numerical results and the corresponding experimental measurements conducted in a corneal epithelium by Giguere et al. [18] are plotted in Fig. 1. The laser focal volume is estimated as $\pi w_0^2z_R=4580\,\mu^3$. The free-electron density of a single electron existing in the focal volume is calculated as $2.18\times10^8\,\mathrm{cm}^{-3}$ which yields a fraction of seed free-electron density to critical free-electron density as $\rho_0/\rho_{cr}=1.25\times10^{-13}$. As shown in Fig. 1, the ablation thresholds predicted by the numerical model with the assumption that a single free electron in the focal volume generates avalanche ionization deviate increasingly from the experimental data with either increasing t_p for $t_p>1$ ps or decreasing t_p for $t_p<1$ ps. For pulses of picoseconds or nanoseconds the current result is consistent with the well-known phenomenon that multiphoton ionization is critical. For pulses of sub-picosecond or femtoseconds, however, it was thought that avalanche ionization predominated and a single free electron might generate avalanche ionization. Clearly, Fig. 1 shows that a single free electron would not trigger avalanche ionization and leads to the occurrence of ablation for sub-picosecond lasers. It requires a certain number of seed electrons (or say the density must be over a critical value which is greater than the density with only one free electron) to trigger the cascade avalanche ionization, leading to plasma-mediated ablation.

Fig. 2 shows the time evolution of free electrons generated by a single laser pulse in a corneal epithelium tissue, based on the numerical modeling of the complete rate equation. The laser parameters are $t_p=100$ fs and $\lambda=800$ nm. The laser fluence is at the experimental measured threshold $F_{th}=1.23\,\mathrm{J/cm}^2$ [18]. We first assume that one free electron in the focal volume (i.e., $\rho_0/\rho_{cr}=1.25\times10^{-13}$) will initiate the avalanche ionization. As illustrated by the solid curve in the figure, the free-electron density will be developed to go over substantially the critical free-electron density ρ_{cr} (i.e., $\rho/\rho_{cr}\gg1$) before the pulse duration ends, which breaks down the precondition that the ablation just occurs because the laser intensity is at the threshold (i.e., ρ/ρ_{cr} can only reaches to unity). By taking our proposed postulate that avalanche ionization occurs after a certain number of free electrons are accumulated, a critical seed free-electron fraction $\rho_0/\rho_{cr}=1.075\times10^{-3}$ is obtained. This value is actually 10 orders of magnitude larger than that assuming only one free electron. Using this critical seed free-electron density value, the time evolution of free electrons is

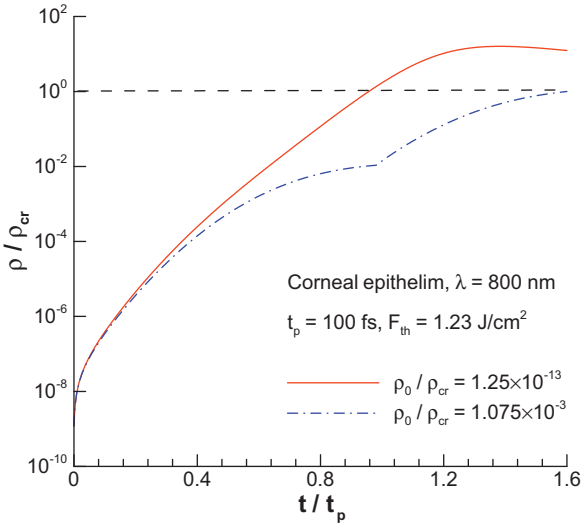

Fig. 2. Evolutions of the free-electron density at threshold fluence with two different critical seed free-electron densities for triggering avalanche ionization.

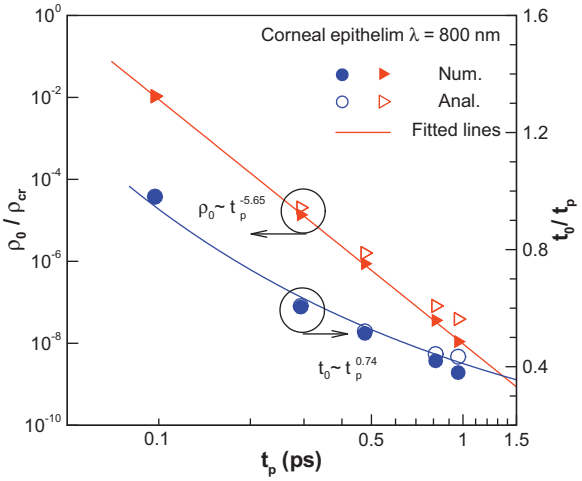

Fig. 4. Comparison of the seed free-electron density and avalanche triggering time between the analytical and numerical predictions for ablation in corneal epithelium at λ = 800 nm with various ultrashort pulse widths.

re-calculated and shown in the dot–dash curve in Fig. 2. Now ablation occurs exactly at the end of the pulse. It means that the fluence is at the threshold value and matches with the experimental measurement.

Fig. 3 shows the temporal evolutions of the free-electron density and the ionization/loss rates in a corneal epithelium tissue subjected to a pulse of $t_p = 100$ fs at 800 nm with threshold irradiation that is experimentally measured as $F_{th} = 1.23$ J/cm^2 [14]. It compares the predictions between the numerical modeling and the analytical solution. The analytical model assumes two separate multiphoton and avalanche ionization processes as described by Eqs. (7) and (9). The critical seed free-electron density is determined by the analytical solution as shown in Fig. 2. In the numerical modeling, the fourth-order Runge-Kutta method was adopted to solve Eq. (1) which incorporates all the four mechanisms simultaneously. Initially there is no free electron, and the time step is chosen as 0.5 fs. From Fig. 3, it is seen that the analytical solutions (free-electron density and two ionization rates) match well with the corresponding results yielded by the complete numerical model. The losses from diffusion and recombination are much smaller than the multiphoton ionization rate before the occurrence of avalanche ionization; and during the avalanche ionization

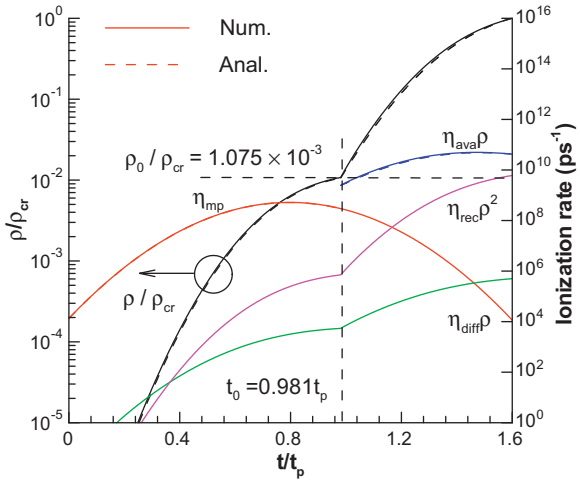

Fig. 3. Evolutions of the free-electron density and ionization/loss rates in corneal epithelium subjected to threshold irradiation with $t_p = 100$ fs and λ = 800 nm.

process these losses are much smaller than the avalanche ionization rate. Thus, the loss mechanisms are negligible in the case studied. Fig. 3 demonstrates that the initial free electrons grow slowly by the multiphoton ionization. Once the free-electron density reaches to the level $\rho_0/\rho_{cr} = 1.075 \times 10^{-3}$ at $t_0 = 0.981t_p$, the avalanche ionization starts and immediately dominates the production of the free electrons until the occurrence of ablation. The results in Fig. 3 validate the postulate introduced in the simplification of the analytical model.

Fig. 4 compares the predictions of the critical seed free-electron density ρ_0 and avalanche triggering time t_0 for various pulse widths by the simplified analytical model and the complete numerical model. For each pulse width the irradiance is at its corresponding threshold value. It is observed that the critical seed free-electron density ρ_0 generally obeys a $t_p^{-5.65}$ rule and decreases as the pulse width increases. As the pulse width increases, the avalanche triggering time t_0 shifts to the pulse head (i.e., t_0/t_p becomes smaller); but follows a relationship, $t_0 \sim t_p^{0.74}$, i.e. the triggering takes longer time. The increase of t_0 leads to increased collision events of the generated free electrons because the collision time τ is a constant; and thus, reduces the critical seed free-electron density for triggering avalanche ionization. We know that IBA requires a finite time, $\tau_{iba} = k\tau$. At λ = 800 nm, $k = 6$, so that $\tau_{iba} = 1.7 \times 6 = 11.2$ fs. Since a sequence of IBA processes are required to induce avalanche ionization, the width of pulse that can induce avalanche ionization ablation must be much greater than τ_{iba}.

From Fig. 4, it is further seen that the simplified exact solution starts to deviate from the complete numerical model when $t_p > 0.5$ ps. To elucidate this upper limit for multiphoton ionization induced avalanche ionization, Fig. 5 shows the evolutions of the free electrons with three different pulse widths ($t_p = 100$ fs, 1.91 and 2.9 ps). The experimentally measured thresholds are $F_{th} = 1.23$, 2.27 and 2.8 J/cm^2 for these three pulses [18], respectively. The results in Fig. 5 are based on the complete numerical modeling. It is observed that the time at ablation occurrence is $1.593t_p$, $1.44t_p$ and $1.486t_p$, for the three pulses, respectively. When $t_p = 2.9$ ps, the recombination loss rate goes over the avalanche ionization rate at an early time $t = 1.44t_p$ before the end of pulse. It implies that the pulse energy is not fully utilized to ionize the material into plasmas even though a threshold value is used and the mechanism of ablation is probably mixed by avalanche ionization and thermal heating. While the ablation occurrence time for the shorter pulse ($t_p = 100$ fs) is very close to the end of pulse ($t_d = 1.5939t_p$). It means

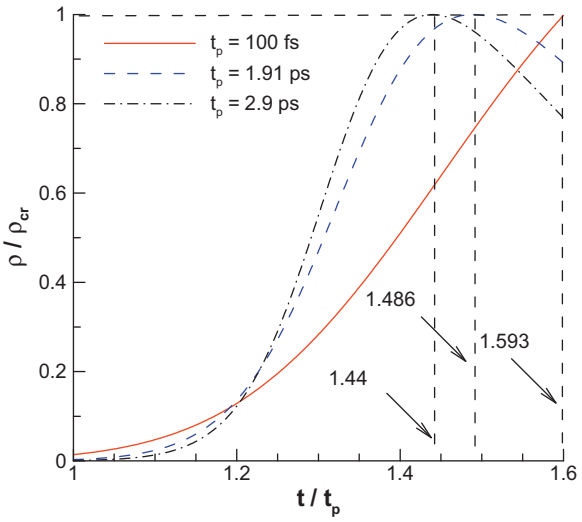

Fig. 5. Evolutions of the free electrons induced by 100 fs, 1.91 ps and 2.9 ps pulses.

that the whole pulse energy is utilized for the multiphoton and avalanche ionizations. Thus, Fig. 5 further confirms that the upper limit for using the simplified analytical model is about 1 ps. It should be pointed out that the recombination coefficient could affect the value of this upper limit and a fixed value was adopted in this study.

Finally the present model is extended to predict ablation crater size in plasma-mediated ablation of PDMS. The pulse width in the experiment [3] conducted by one of the co-authors and his student was $t_p = 900$ fs and the wavelength was $\lambda = 1552$ nm. The focal spot size for the laser beam was about $2w_0 = 8\,\mu$m. The experimentally determined ablation threshold is $F_{th} = 4.6\,\text{J/cm}^2$. Using the present analytical solution, the critical seed free-electron density and the avalanche triggering time are determined to be $\rho_0 = 3.6 \times 10^{20}\,\text{cm}^{-3}$ and $t_0 = 1.5867 t_p$, respectively. This critical seed free-electron density is then set as a triggering point to initiate avalanche ionization at each location in the laser impinging area. The evolution of the free electrons density at every point on the PDMS surface is numerically modeled by employing Eq. (1) with the analytically determined critical seed free-electron density. Plasma-mediated ablation occurs at locations where the free electrons density in the simulation is not less than the critical free-electron density, $\rho_{cr} = 4.63 \times 10^{20}\,\text{cm}^{-3}$. The crater boundary is where the free electron density equals to this critical value. Fig. 6 compares the crater diameters predicted with the combination of the present analytical and numerical models with those determined experimentally [3]. It is seen that the present results yield a good quantitative agreement with the experimental measurements. This further validated our model and postulate.

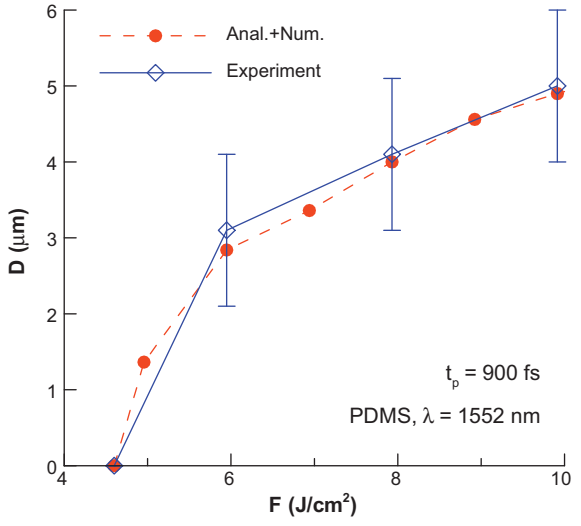

Fig. 6. Comparison of crater size on PDMS between the analytical prediction and the experimental measurements [3].

4. Conclusion

In summary, we obtained an analytical solution for free-electron evolution in plasma-mediated ablation of transparent media based on the postulate that a critical seed free electron density exists for triggering avalanche ionization and the ionization process can be split into two separate processes with different dominant mechanism. The theoretical model is validated via comparisons with the experimental measurements of ablation threshold in a corneal epithelium tissue and of ablation crater sizes in a transparent PDMS. A complete numerical model with all the ionization and loss mechanisms is also employed in the comparison to elucidate and validate the conditions when avalanche ionization occurs and dominates in the plasma-mediated laser ablation process. The proposed model is useful for ablation with ultrashort pulses in the sub-picosecond range. As the pulse width increases, the critical seed free-electron density decreases, obeying a $t_p^{-5.65}$ rule for ablation in the corneal epithelium studied.

References

[1] A. Chimmalgi, T.Y. Choi, C.P. Grigoropoulos, K. Komvopoulos, Femtosecond laser aperturless near-field nanomachining of metals assisted by scanning probe microscopy, Appl. Phys. Lett. 82 (2003) 1146–1148.
[2] C. Cheng, X. Xu, Mechanisms of decomposition of metal during femtosecond laser ablation, Phys. Rev. B 72 (2005), 165415.
[3] H. Huang, Z. Guo, Ultra-short pulsed laser PDMS thin-layer separation and micro-fabrication, J. Micromech. Microeng. 19 (2009), 055007.
[4] Z. Guo, X.L. Wang, H. Huan, Plasma-mediated ablation of biofilm contamination, Appl. Surf. Sci. 257 (2010) 1247–1253.
[5] Z. Zhang, G. Gogos, Theory of shock wave propogation during laser ablation, Phys. Rev. B 69 (2004) 235403.
[6] C.-H. Fan, J.P. Longtin, Modeling opitcal breakdown in dielectrics during ultrafast laser processing, Appl. Opt. 40 (2001) 3124–3131.
[7] A.V. Rode, E.G. Gamaly, B. Luther-Davies, B.T. Taylor, J. Dawes, A. Chan, R.M. Lowe, P. Hannaford, Subpicosecond laser ablation of dental enamel, J. Appl. Phys. 92 (2002) 2153.
[8] H. Huang, Z. Guo, Human dermis separation via ultra-short pulsed laser plasma-mediated ablation, J. Phys. D: Appl. Phys. 42 (2009), 165204.
[9] X.L. Wang, Z. Guo, Effective removal of adhering cells via ultrashort laser pulses, Opt. Laser Technol. 42 (2010) 447–451.
[10] H. Campell, F. Rainer, M.R. Kozlowski, C.R. Wolfe, I.M. Thomas, F.P. Milanovich, Damage resistant optics for a mega-joule solid-state laser, SPIE 1441 (1990) 444–456.
[11] D. Du, X. Liu, G. Korn, J. Squire, G. Mourou, Laser-induced breakdown by impact ionization in SiO_2 with pulse widths from 7 ns to 150 fs, Appl. Phys. Lett. 64 (1994) 3071–3073.
[12] B.C. Stuart, M.D. Feit, S. Herman, A.M. Rubenchik, B.W. Shore, M.D. Perry, Nanosecond-to-femtosecond laser-induced breakdown in dielectrics, Phys. Rev. B 53 (1996) 1749–1761.
[13] A. Tien, S. Backus, H. Kapteyn, M. Murnane, G. Mourou, Short-pulse laser damage in transparent materials as a function of pulse duration, Phys. Rev. Lett. 82 (1999) 3883–3886.
[14] M.D. Feit, A.M. Komashko, A.M. Rubenchik, Ultra-short pulse laser interaction with transparent dielectrics, Appl. Phys. A 79 (2004) 1657–1661.
[15] J. Noack, A. Vogel, Laser-induced plasma formation in water at nanosecond to femtoseconds time scales: calculation of thresholds absorption coefficients, and energy density, IEEE J. Quantum Electron. 35 (1999) 1156–1167.
[16] A. Vogel, J. Noack, G. Hüttmann, G. Paltauf, Mechanisms of femtoseconds laser nanosurgery of cells and tissues, Appl. Phys. B 81 (2005) 1015–1047.
[17] J. Jiao, Z. Guo, Modeling of ultra-short pulsed laser ablation in water and biological tissues in cylindrical coordinates, Appl. Phys. B 103 (2011) 195–205.
[18] D. Giguere, G. Olivie, F. Vidal, S. Toetsch, G. Girard, T. Ozaki, J.C. Kieffer, O. Nada, I. Brunette, Laser ablation threshold dependence on pulse duration for fused

silica and corneal tissues: experiments and modeling, J. Opt. Soc. Am. A: Opt. Image Sci. Vis. 24 (2007) 1562–1568.
[19] L.V. Keldysh, Ionization in the field of a strong electromagnetic wave, Sov. Phys. JETP 20 (1965) 1307–1314.
[20] P.K. Kennedy, A first-order model for computation of laser-induced breakdown thresholds in ocular and aqueous media: Part I-Theory, IEEE J. Quantum Electron. 31 (1995) 2241–2249.
[21] Q. Sun, H. Jiang, Y. Liu, Z. Wu, H. Yang, Q. Gong, Measurement of the collision time of dense electronic plasma induced by a femtosecond laser in fused silica, Opt. Lett. 30 (2005) 320–322.
[22] F. Docchio, Lifetimes of plasmas induced in liquids and ocular media by single Nd:YAG-laser pulses of different duration, Europhys. Lett. 6 (1988) 407–412.
[23] A. Karczemska, A. Sokolowska, Materials for DNA sequencing chip, J. Wide Bandgap Mater. 9 (2002) 243–259.